



Cite this: *Sustainable Food Technol.*, 2025, 3, 1114

## Fabrication of gel-like sorbents derived from pomelo (*Citrus grandis* L.) peel powder via an immediate setting emulsion approach†

Haoxin Wang,<sup>a</sup> Peng Wang,<sup>b</sup> Stefan Kasapis<sup>a</sup> and Tuyen Truong   \*ac

This study developed emulsion gel-like sorbents by valorising pomelo peel (*Citrus grandis* L.) powder enriched with fibres (52.11–59.59%) and antioxidants. The process utilized an emulsion-based gelation approach, where an immiscible oil–water mixture with various oil-to-water ratios (1:3, 1:1, and 3:1) was first blended with a pre-emulsion using high-shear mixing. PP powder (10–40% w/w) with two particle sizes (125 and 250 µm) was then incorporated into the pre-emulsion, where its amphiphilic nature enabled interactions with both the oil and water phases, stabilising the emulsion and promoting gelation. Upon mixing, the PP powder rapidly absorbed the oil and water phases, forming self-sustaining gel-like sorbents within 2 min at room temperature. Comprehensive analyses of their chemical composition, antioxidant properties, texture, rheology, microstructure, and oxidative stability showed that increasing the water phase reduced the amount of PP powder required, softened the sorbents, and enhanced their cohesiveness. Conversely, higher PP concentrations and oil phases increased the gel strength and textural hardness by forming denser structures and altering oil droplet sizes. Stability testing revealed that oil-rich sorbents (3:1 oil-to-water ratio) maintained a peroxide value below 4 meq kg<sup>-1</sup>, attributed to their low water content and the antioxidant-rich properties of PP powder. This research provides a robust and eco-friendly approach to developing functional and stable PP-based sorbents, with potential applications as fat replacers for creating low-fat food products.

Received 28th January 2025  
Accepted 1st May 2025

DOI: 10.1039/d5fb00027k  
[rsc.li/susfoodtech](http://rsc.li/susfoodtech)

### Sustainability spotlight

The global challenge of reducing food waste and developing sustainable alternatives to high-fat food products aligns with the need for innovative, eco-friendly solutions. This study addresses these issues by valorising pomelo peel, a common agricultural byproduct, into gel-like sorbents with potential applications as fat replacers in low-fat food formulations. Using an emulsion-based gelation approach, the research not only reduces waste but also promotes resource efficiency by leveraging the natural amphiphilic and antioxidant properties of pomelo peel powder. This work directly supports UN Sustainable Development Goal (SDG) 12 (Responsible Consumption and Production) by encouraging circular economy practices and SDG 3 (Good Health and Well-being) by providing healthier food options. It offers a scalable pathway for sustainable food production.

## 1 Introduction

Gels are widely used in the food industry for various purposes, such as thickening, stabilising, and gelling. Emulsion gelling is an efficient oil structuring strategy that stabilises oil–water mixtures using gelators to crosslink and create a three-

dimensional (3D) structure to trap oil, resulting in the formation of emulsion-based gels.<sup>1</sup> Emulsion gels are typically made from gelators, water and oil with their properties significantly influenced by gelling methods including heating, cooling, pH adjustments, enzymatic treatments, and salt addition.<sup>2,3</sup> They show great potential as fat replacers due to their inherent emulsion properties, offering superior juiciness and hardness compared to traditional starch-based fat replacers while reducing the oil content.<sup>1,4</sup>

Although emulsion gels are widely studied, their fabrication still faces certain limitations, with one of the most critical factors being the requirement of prolonged heating time.<sup>5,6</sup> At present, almost all gelators (e.g., polysaccharides, protein, and starch) rely on heating to form 3D structures. However, prolonged heating duration negatively impacts both oil and water phases, leading to fat oxidation, water droplet coalescence, and

<sup>a</sup>School of Science, STEM College, RMIT University, Melbourne, Australia. E-mail: [tuyen.truong@rmit.edu.au](mailto:tuyen.truong@rmit.edu.au); [s3470758@student.rmit.edu.au](mailto:s3470758@student.rmit.edu.au); [Stefan.kasapis@rmit.edu.au](mailto:Stefan.kasapis@rmit.edu.au)

<sup>b</sup>Nanjing Agricultural University, Key Laboratory of Meat Processing and Quality Control, College of Food Science and Technology, Nanjing, 210095, PR China. E-mail: [wpeng@njau.edu.cn](mailto:wpeng@njau.edu.cn)

<sup>c</sup>School of Science, Engineering and Technology, RMIT Vietnam, Ho Chi Minh City, Vietnam

† Electronic supplementary information (ESI) available. See DOI: <https://doi.org/10.1039/d5fb00027k>



phase separation.<sup>3,7</sup> Minimising the heating treatment is one of the feasible approaches to mitigate these adverse effects. Therefore, developing non-thermal methods for setting emulsion gels is crucial to maintain their functional and nutritional properties while also reducing energy consumption.

Plant by-products rich in phenolic compounds and cost-effective are valuable materials generated from food processing.<sup>8</sup> However, they remain largely underutilised and are primarily used as animal feed. Previous studies have shown that these plant-based materials, including bamboo, apple pomace, corn cob, and citrus peels, can naturally function as amphiphilic sorbents, forming gels through the amphiphilicity of the side chain and porous structure of the particles.<sup>9–13</sup> Most of these studies employed high concentrations of gelators and large particle sizes, which may negatively affect the sensory properties and digestibility of the resulting gels.<sup>10,14</sup> In addition, most studies focused on plant waste absorbing either water or oil as the solvent, leaving out the potential of plant waste to form emulsion gels, combining both oil and water phases, largely unexplored and in need of further investigation for application in functional food systems.

Pomelo (*Citrus grandis* L.), the largest citrus fruit, generates substantial peel waste, with approximately 2.1 million tons discarded annually from global production.<sup>15</sup> Pomelo peels (PPs) are rich in antioxidants and can help alleviate chronic diseases such as type 2 diabetes and cancer.<sup>16</sup> Due to the porous structure and amphiphilic properties of pomelo peels, they can be used as a natural gelator. Our previous study demonstrated the formation of oleogel-like and hydrogel-like sorbents from PP powders (10–40% w/w) by mixing with oil and distilled water, respectively, for two minutes without heating. The oleogel-like sorbents required a higher PP content (25–35%) compared to hydrogel-like sorbents (10–20%).<sup>13</sup> The findings revealed that the gelling mechanism is driven by the high fibre content of PP and the interactions between powder particles and solvent droplets. Utilising an emulsion-based approach to develop PP-based sorbents can further enhance health benefits by reducing the oil content while offering greater flexibility in tailoring the gel-like sorbents' properties through varying oil-to-water ratios to achieve desired functionality.

This study employs an emulsion-based gelation process in which an immiscible oil–water mixture is transformed into a pre-emulsion through high-shear mixing (*e.g.*, using an Ultra-Turrax homogeniser). Pomelo peel powder is then added to the pre-emulsion. The amphiphilic nature of the PP powder facilitates interactions with both the oil and water phases, stabilising the emulsion and initiating gelation. The influence of varied oil : water ratios and PP powder particle size (125 µm and 250 µm PP) was examined. Comprehensive analyses of the physico-chemical characteristics, microstructure, and oxidative stability of the resulting sorbents were carried out to examine the mechanisms of sorbent formation and identify the key factors influencing the properties of PP-based sorbents. The knowledge gained will contribute to the understanding of the gelling mechanisms of PP-based sorbents and the identification of optimal conditions for emulsion-based/gel-like sorbent formation. The outcomes of this study will provide an eco-friendly

approach to valorising agricultural byproducts, enabling the development of healthier, low-fat food products by using PP-based sorbents as potential fat replacers for processed meat, baked goods and confectionery while meeting industry demands for sustainable production practices.

## 2 Materials and methods

### 2.1 Materials

Whole pomelo fruits and rice bran oil were purchased from the local market (Melbourne, Victoria, Australia). All chemicals, including Nile red, butanol, hexane, ammonium thiocyanate, *p*-anisidine, glacial acetic acid, isoctane, iron(III) chloride (FeCl<sub>3</sub>) and fluorescein isothiocyanate isomer I (FITC) were acquired from Sigma (Burlington, USA). All chemicals were of analytical grade.

### 2.2 Preparation of pomelo peel (PP) powder

As described by Wang *et al.*,<sup>13</sup> the pomelo peels were manually dehulled and cut into 2–3 cm pieces using a knife. The pomelo peels were then dried in an oven (Ezzi Vision, Chirnside Park, Australia) at 70 °C for 72 h. The dried pomelo peels (less than 5% w/w moisture) were ground using an ultra-grinding cycle in a Ninja Auto-IQ food processor (Mann & Noble, NSW, Australia) for 2 min and passed through 250 µm and 125 µm sieves to obtain 2 fractions of different sizes, denoted as 250 µm and 125 µm powders, respectively. The powders' particle sizes were measured using a Mastersizer 3000 (Malvern Ltd, Malvern, UK). The resulting pomelo peel powder was carefully packed in sealed plastic bags and stored at –20 °C until further analyses. Our previous study detailed the chemical composition of pomelo peel powder with 7.44–9.86% starch, 7.96–8.63% protein, 2.48–2.68% ash, and 52.11–59.59% fibres. The 250 µm PP powder contains 23.91% insoluble fibres, comprising 15.72% cellulose, 8.11% hemicellulose, and 0.09% lignin, while the soluble fibre content is 28.20%. Similarly, the 125 µm PP powder has a higher insoluble fibre content of 25.43%, consisting of 19.35% cellulose, 5.98% hemicellulose, and 0.10% lignin, with a soluble fibre content of 34.16%.<sup>13</sup>

### 2.3 Chemical and microstructural characterisation of PP powders

**2.3.1 Phenolic content.** The phenolic fragments were extracted following the method described by Singleton & Rossi,<sup>17</sup> as adapted from Wang *et al.*<sup>18</sup> One gram PP powder was immersed in 45 mL methanol and water bathed at 60 °C for 2 h. The mixture was then centrifuged in a Beckman centrifuge (Indianapolis, USA) at 2500g for 10 min. The process was repeated three times; the supernatant was collected and evaporated by a rotary vacuum concentrator (Martin Christ, Osterode, Germany) to dryness at 45 °C. Then, the phenolic fragment was redissolved in 10 mL methanol and stored at –20 °C until measurement. The phenolic fragments were diluted 10 times during analysis.

**2.3.2 Total phenolic content (TPC).** TPC determination was done following the method of Singh *et al.*<sup>19</sup> with minor modifications. One hundred microliter phenolic fragment was mixed



with 200  $\mu\text{L}$  of 10% v/v Folin–Ciocalteu reagent and 800  $\mu\text{L}$  of 7.5% w/v  $\text{Na}_2\text{CO}_3$ . The mixture was then heated to 60  $^{\circ}\text{C}$  for 30 min using a water bath. The absorbance was measured at 765 nm using a CLARIOstar® microplate reader (BMG Labtech, Ortenberg, Germany) with gallic acid as the standard. The TPC value was expressed as milligrams of gallic acid equivalent per gram ( $\text{GAE } \mu\text{g g}^{-1}$ ).

**2.3.3 Total flavonoid content (TFC).** TFC was determined by a method reported by Singh *et al.*<sup>19</sup> The phenolic fragment (100  $\mu\text{L}$ ) was combined with 300  $\mu\text{L}$  of 80% (v/v) methanol, 20  $\mu\text{L}$  of 10% (w/v) aluminum chloride, and 20  $\mu\text{L}$  potassium acetate in the dark for 10 min. The mixture was then diluted with 560  $\mu\text{L}$  distilled water, allowed to react in the dark for 30 min and then measured using a CLARIOstar® microplate reader at 415 nm. Rutin was used to generate the standard curve for quantification. The TFC value was expressed as milligrams of rutin equivalent per gram ( $\text{RTE } \mu\text{g g}^{-1}$ ).

**2.3.4 Scanning electron microscopy (SEM).** The microstructure of PP powders of different particle sizes was observed with a FEI Quanta 200 SEM system (FEI Company, Hillsboro, OR, USA). The microscope was set in high vacuum mode and operated at a voltage of 15 kV and with a spot size of 2.5. The magnification was set from 300 times to 2000 times.

## 2.4 Preparation of gel-like structures by mixing PP powder with pre-emulsions

The gel-like structures were prepared by first creating a pre-emulsion, an intermediate mixture of oil and water, which was then gelled by incorporating pomelo peel (PP) powder. To form the pre-emulsion, rice bran oil was mixed with water at ratios of 1 : 3, 1 : 1, and 3 : 1 using a T-25 digital Ultra-Turrax homogeniser (IKA Asia, Selangor, Malaysia) at 15 000 rpm for 15 min, resulting in a milky solution. The pre-emulsions, with fixed oil to ratios, were immediately combined with a pre-weighted amount of PP powder (125  $\mu\text{m}$  and 250  $\mu\text{m}$ ) at concentrations in the range of 10–40%. The mixture was manually stirred for 1 min and vortexed for an additional minute. If gelling was successful, the emulsion gels were set immediately without any standing time.

A total of 42 samples were produced (with 3 oil : water ratios  $\times$  7 PP powder concentrations (10, 15, 20, 25, 30, 35, and 40% w/w)  $\times$  2 particle sizes) in which 15 samples were self-sustained. Additionally, 100% rice bran oil mixed with 30% and 35% PP powder was used as a control to produce oleogel-like sorbents, based on a previous study by Wang *et al.*<sup>13</sup> These concentrations were chosen to ensure the formation of self-sustaining gels. After preparation, all sorbents were left to stand at room temperature for 2 hours before further analyses. Detailed compositional data and sample names are provided in Appendix 1. The self-sustained sorbent samples are labelled based on the particle size of the PP powder and their respective PP concentrations. Samples made from 125  $\mu\text{m}$  PP powder are denoted as 125  $\mu\text{m}$ -S1, -S2, -S3, -S4, -S5, -S6, -S7, and -S8, while those made from 250  $\mu\text{m}$  PP powder are labelled as 250  $\mu\text{m}$ -S1, -S2, -S3, -S4, -S5, -S6, and -S7. Each label corresponds to a specific PP concentration used in the formulation.

## 2.5 Characterisation of gel-like sorbent samples

**2.5.1 Oil loss.** A subsample weighing 1.5 g ( $w_0$ ) was transferred to a 2 mL centrifugation tube and centrifuged for 15 min at 10 000 rpm using a Sigma 1–14k centrifuge (John Morris Group, Deepdene, Australia). The excess solvent was then removed, and the remaining sample was weighed ( $w_1$ ). The percentage of oil loss was calculated using the following formula:

$$\frac{w_0 - w_1}{w_0} \times 100\% \quad (1)$$

in which  $w_0$  is the initial weight of sorbent and  $w_1$  is the weight of sorbent after oil removal.

**2.5.2 Texture profile analysis (TPA).** The texture analysis of the sorbent samples was conducted using a TA.XTplusC texture analyser (Stable Micro Systems, Godalming, UK) according to the method of Wang *et al.*<sup>12</sup> First, the sorbent samples were filled into a 34  $\times$  12 mm round mould, then trimmed, and left to stand for 10 min. Then, a double compression program was implemented on the sorbents using a 45 mm round compression probe. The compression speed was set at 1.0  $\text{mm s}^{-1}$ , and the depth was 9 mm and 6 mm for the first and second cycles, respectively. The texture profile analysis (TPA) curves were generated using the Exponent software version 6.1.23.0 (Stable Micro Systems, Godalming, UK), from which hardness ( $N$ ) and cohesiveness (%) values were calculated.

## 2.6 Rheological behaviour

Oscillation strain sweep and frequency sweep tests were carried out with a DHR-2 hybrid rheometer (TA Instruments, New Castle, USA) with a 40 mm parallel plate and a geometry gap of 1.2 mm.<sup>12</sup> Amplitude stress sweeps were used to determine the linear viscoelastic range, and frequency sweeps (1–1000  $\text{rad s}^{-1}$  with an increment of 10  $\text{rad s}^{-1}$ ) were used to determine the stress value within the range.

## 2.7 Microstructural analysis

**2.7.1 Bright-field microscopy.** Bright-field microscopy was used to investigate the morphological features of the sorbents. A fine smear of sorbents was placed on a slide and covered with a glass slide. The sample was observed under an ECLIPSE Ci POL polarised light microscope (Nikon, Tokyo, Japan) in normal mode. The images were recorded with a D610 digital camera (Nikon, Tokyo, Japan) at 200 $\times$  magnification.

**2.7.2 Confocal laser scanning microscopy (CLSM).** Rice bran oil and water were distilled with 0.5% Nile Red and FITC, respectively. The sorbents were then prepared following the method described in Section 2.4. A thin layer of sorbents was transferred onto microscopic slides and observed using a Nikon A1R microscope (Nikon, Tokyo, Japan). The samples were excited at wavelengths of 488 nm and 505 nm for Nile Red and FITC, respectively. Images were captured at 40 $\times$  magnification.

## 2.8 Oil droplet size

The oil droplet size was determined following Luo *et al.*<sup>20</sup> Two grams of sorbent sample was mixed with 20 mL of 5 wt% SDS and 50 mM 2-mercaptoethanol. The mixture was shaken



overnight at room temperature, and the mixture was measured with a Mastersizer 3000 (Malvern Ltd, Malvern, UK). The refractive index was set at 1.47 for rice bran oil droplets.

## 2.9 Oxidative stability

Evaluation of the oxidative stability of the resultant sorbents was done following a modified accelerated method of Liu *et al.*<sup>21</sup> The sorbents were placed in 70 mL vials with loose caps and stored in a 50 °C oven for 10 days. The oxidation stability of sorbents was measured on day 0, day 2, day 4, day 6, day 8, and day 10. The sub-samples (0.1 g) were first dissolved in 3 mL hexane and allowed to evaporate at 45 °C for 4 h to dryness using an RVC 2-33 rotary concentrator. The dried oil was used for further analysis.

**2.9.1 Peroxide values.** The primary oxidative products of all sorbents were determined using the peroxide value (PV) according to the method of Liu *et al.*<sup>21</sup> with minor modifications. First, a working solution was prepared by mixing methanol with butanol in a ratio of 2 : 1. Subsequently, 15 mL of the extracted oil was dissolved in 15 mL of the working solution. Furthermore, the diluted oil sample was mixed with 15 µL of ammonium thiocyanate and allowed to stand in the dark for 20 min at room temperature. A standard curve was plotted by replacing the oil with FeCl<sub>3</sub>, while the blank was measured by substituting the oil with the working solution. The final absorbance was obtained at 510 nm using a POLARstar Omega plate reader (BMG Labtech, Mornington, Australia). The results were expressed in 10 meq kg<sup>-1</sup>.

**2.9.2 p-Anisidine value.** To determine the secondary oxidative products, the *p*-anisidine value (PAV) was measured following the method described by Zuo *et al.*<sup>22</sup> In brief, 15 µL of the extracted oil sample was diluted 100 times with isoctane and reacted with 30 µL of 2.5 mg mL<sup>-1</sup> *p*-anisidine in glacial acetic acid. The pure extracted oil was used as a blank. The absorbance was measured at 350 nm using a POLARstar Omega plate reader (BMG Labtech, Mornington, Australia).

## 2.10 Colouration

The colour of the sample during storage was assessed using a GT0167 colorimeter (Gabrielli Technology, Calenzano, Italy). Prior to measurement, a white standard was calibrated with the colorimeter. The samples were then measured five times, and the results were recorded as *L*\* (lightness), *a*\* (redness), and *b*\* (yellowness). The samples were measured on day 0 (day 0) and day 10 (day 10). The total colour difference  $\Delta E$  was calculated as

$$\Delta E = \sqrt{(L^* \text{ day0} - L^* \text{ day10})^2 + (a^* \text{ day0} - a^* \text{ day10})^2 + (b^* \text{ day0} - b^* \text{ day10})^2} \quad (2)$$

## 2.11 Statistical analyses

The entire experiment was conducted in triplicate with each measurement performed at least twice. One-way ANOVA and

Tukey's test ( $p < 0.05$ ) were carried out to compare the differences among samples using Minitab Express (Version 1.2.0, Minitab Pty Ltd, Sydney, Australia). The level of significance was selected as  $p < 0.05$ .

## 3 Results and discussion

### 3.1 Morphological features of the emulsion-based sorbents

Fig. 1 illustrates the appearance of emulsion-based sorbents formed using 125 µm and 250 µm PP powders. These sorbents showed gel-like features due to their self-standing appearance against gravity.<sup>12</sup> At an oil-to-water ratio of 1 : 3, the 125 µm PP powder produced sorbents at 20% (125 µm S1) and 25% (125 µm S2) PP powder contents, respectively. As the oil-to-water ratio increased to 1 : 1 and 3 : 1, sorbents were formed across a wider range of PP powder contents from 15% to 25% (125 µm S3–S8 samples). In contrast, the 250 µm PP powder formed sorbents at 10% to 15% for all oil-to-water ratios: 1 : 3 (250 µm S1–S2 samples), 1 : 1 (250 µm S3–S4 samples), and 3 : 1 (250 µm S5–S6 samples). At a 3 : 1 ratio, 250 µm PP powder can form sorbents at 20% concentration (250 µm S7 sample). These visual observations imply that the 250 µm PP particles may have superior oil/water sorption capacity, and increasing the oil phase enhances their oil/water holding capacity.

Regarding 125 µm sorbents, increasing the oil content reduces the amount of PP powder required to form sorbents. For an oil-to-water ratio of 1 : 3, 20% PP was necessary to form stable sorbents (125 µm S1), whereas 15% PP resulted in a sticky emulsion (125 µm S0, Fig. 1). However, at higher oil-to-water ratios (1 : 1 and 3 : 1), sorbents could form with only 15% PP. Previous studies have shown that a higher oil content can increase the viscosity of solvent mixtures and enhance the gelling capacity and emulsion viscosity.<sup>10,23</sup> However, it is important to note that increasing oil content does not consistently reduce the amount of gelator required to form sorbents. As shown in Fig. 1(G1, G2 & H1), control samples absorbing only rice bran oil required the highest PP concentration (25–35%) to form self-standing sorbents. These sorbents, extensively analysed in our previous study, exhibited gel-like morphology and gravitational resistance. Our previous study reported that PP has an amphiphilic nature but tends to favour water absorption.<sup>13</sup> In water-rich emulsions, saturation limits oil absorption, whereas in oil-rich systems, both water and oil can be absorbed. Besides, the PP is rich in fibres, including pectin and cellulose, which likely contribute to emulsion stability by enhancing its viscosity, steric hindrance, and structural stability.<sup>24,25</sup>

### 3.2 Microstructure of PP powders and the resultant sorbents

Fig. 2 presents SEM images of PP powders having 250 µm and 125 µm particle sizes. The observed microstructure was



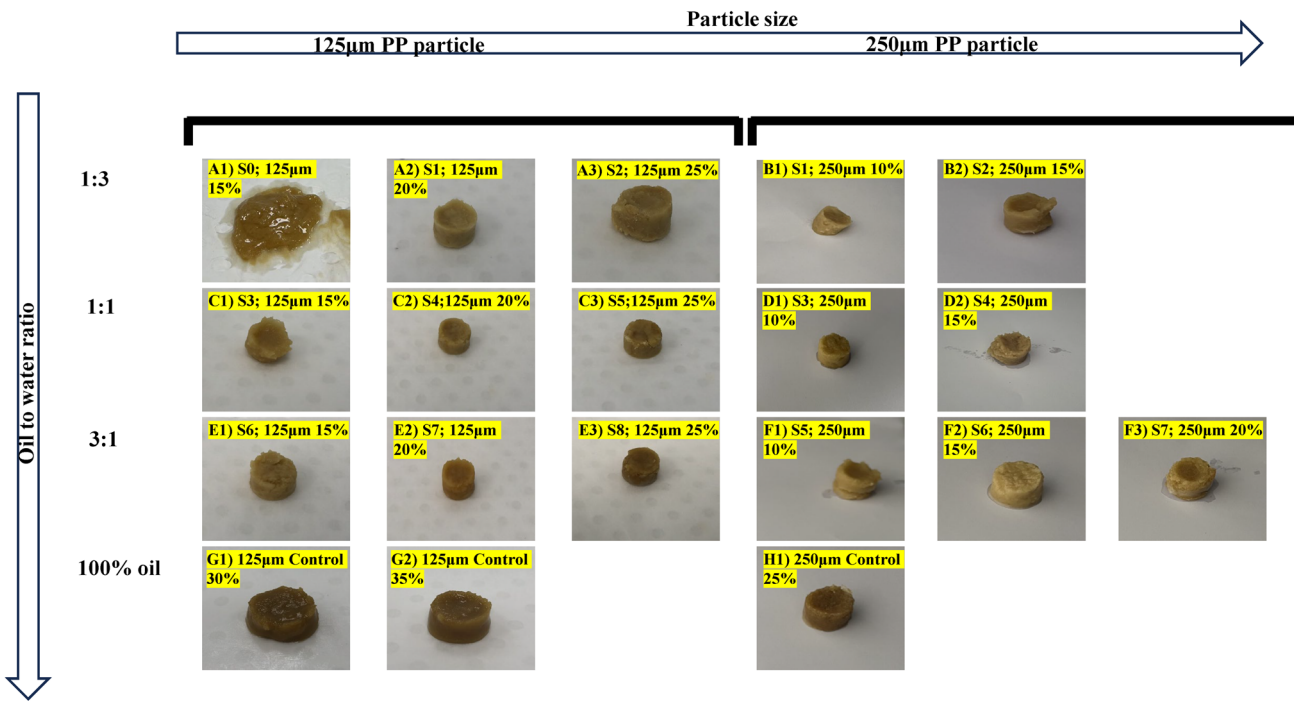


Fig. 1 Visual appearance of sorbents produced using pomelo peel (PP) powders with different particle sizes (125  $\mu\text{m}$  and 250  $\mu\text{m}$ ), oil-to-water ratios (1:3, 1:1, and 3:1), and PP powder concentrations (10–35% w/w). The left three columns represent sorbents formed with 125  $\mu\text{m}$  PP powder, while the right three columns represent those formed with 250  $\mu\text{m}$  PP powder. Five samples correspond to the 1:3 oil-to-water ratio (A1–A3, B1, and B2), five to the 1:1 ratio (C1–C3, D1, and D2), and six (E1–E3 and F1–F3) to the 3:1 ratio. The last row shows oil-only sorbents (control samples). Each subfigure specifies the particle size and PP powder concentration used for the respective sorbents (e.g., "125  $\mu\text{m}$  15%" indicates sorbents made from 125  $\mu\text{m}$  PP powder at a 15% concentration).

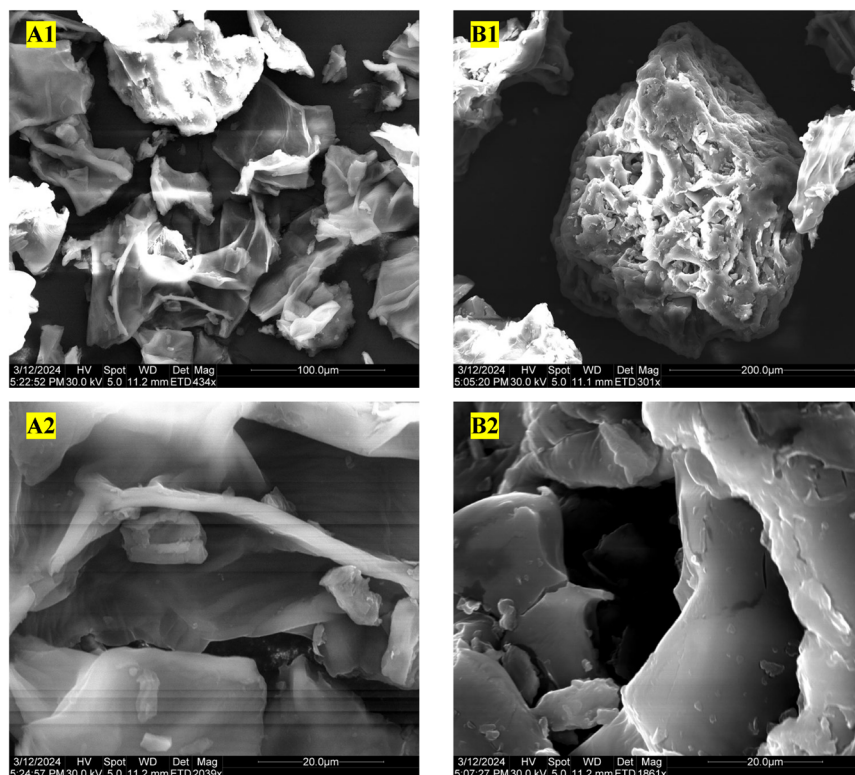


Fig. 2 Scanning electron microscopy (SEM) images of pomelo peel (PP) particles of different sizes, with 125  $\mu\text{m}$  PP particles shown at 400 $\times$  magnification (A1) and 2000 $\times$  magnification (A2) and 250  $\mu\text{m}$  PP particles at 300 $\times$  magnification (B1) and 1800 $\times$  magnification (B2); the scale bars represent 100  $\mu\text{m}$  (A1), 20  $\mu\text{m}$  (A2), 200  $\mu\text{m}$  (B1), and 20  $\mu\text{m}$  (B2).



consistent with previous studies that the 250  $\mu\text{m}$  PP particles exhibit a more complete honeycomb structure, which enhances their ability to attract and retain water and oil.<sup>12,26</sup> Additionally, the micrographs reveal that the surface of the 250  $\mu\text{m}$  PP particles (Fig. 2B) is rougher compared to that of the 125  $\mu\text{m}$  PP particles (Fig. 2A). Mahmoud<sup>27</sup> studied the oil absorption properties of flax fibres and found that fibres with rough surfaces containing small pores can increase oil retention by enhancing the oil trapping efficiency. The rougher surface also increases frictional forces, which aids in retaining oil droplets. This explains the higher overall sorption rate of 250  $\mu\text{m}$  PP particles than their 125  $\mu\text{m}$  counterpart.

Both light microscopy (Fig. 3) and CLSM (Fig. 4) were used to characterise the microstructure of the resultant sorbents. In Fig. 3, the 250  $\mu\text{m}$  sorbents show an accumulation of large aggregates which exhibit more particle-to-particle interactions, whereas the 125  $\mu\text{m}$  sorbents show a small but uniform structure which displays greater particle-to-droplet interactions, consistent with previous studies.<sup>10,12</sup> The 125  $\mu\text{m}$  sorbents also show a continuous tendency of droplet-to-particle conversion. However, when the PP powder particles became larger (250  $\mu\text{m}$  sorbents), the structure shows more dispersion at low PP concentrations (Fig. 3(B1 & B2)). This indicates a reduction in particle-to-particle interaction. It was reported that the oil/water droplets can increase droplet-to-droplet interactions, which enhances the gelation process.<sup>5</sup> Therefore, introducing a water phase into the oil phase can reduce the amount of PP powder required to form a gel.

CLSM images (Fig. 4) of the resultant sorbents provide valuable insights into their microstructure, with red indicating the oil phase, green representing the water phase, and black corresponding to the pomelo peel (PP) powder. The PP particle size examined in this study is relatively large, limiting the ability to view the overall microstructure of the sorbents and instead focusing on selected internal structures. Overall, sorbents prepared from 125  $\mu\text{m}$  PP exhibited smaller droplet sizes and more uniform microstructures, indicating less phase dispersion, particularly at a 1 : 1 oil-to-water ratio. In contrast, sorbents made from 250  $\mu\text{m}$  PP showed greater aggregation with great phase separation, likely due to reduced interfacial interaction of larger particles.

Compared to traditional emulsion gels, which typically display distinct water and oil phases, the sorbents formed through the emulsion-based approach exhibited a more intertwined microstructure.<sup>4</sup> The oil and water phases appeared more closely integrated, likely due to the amphiphilic nature of the PP powder and the dynamic interactions during the emulsion setting process.<sup>12</sup> This interwoven microstructure may contribute to enhanced stability and unique functional properties, making these sorbents a promising alternative for applications requiring integrated oil–water systems.<sup>28</sup>

### 3.3 Textural and rheological behaviour

Table 1 presents selected TPA values of the produced sorbents. Overall, the inclusion of water in the form of an immediate

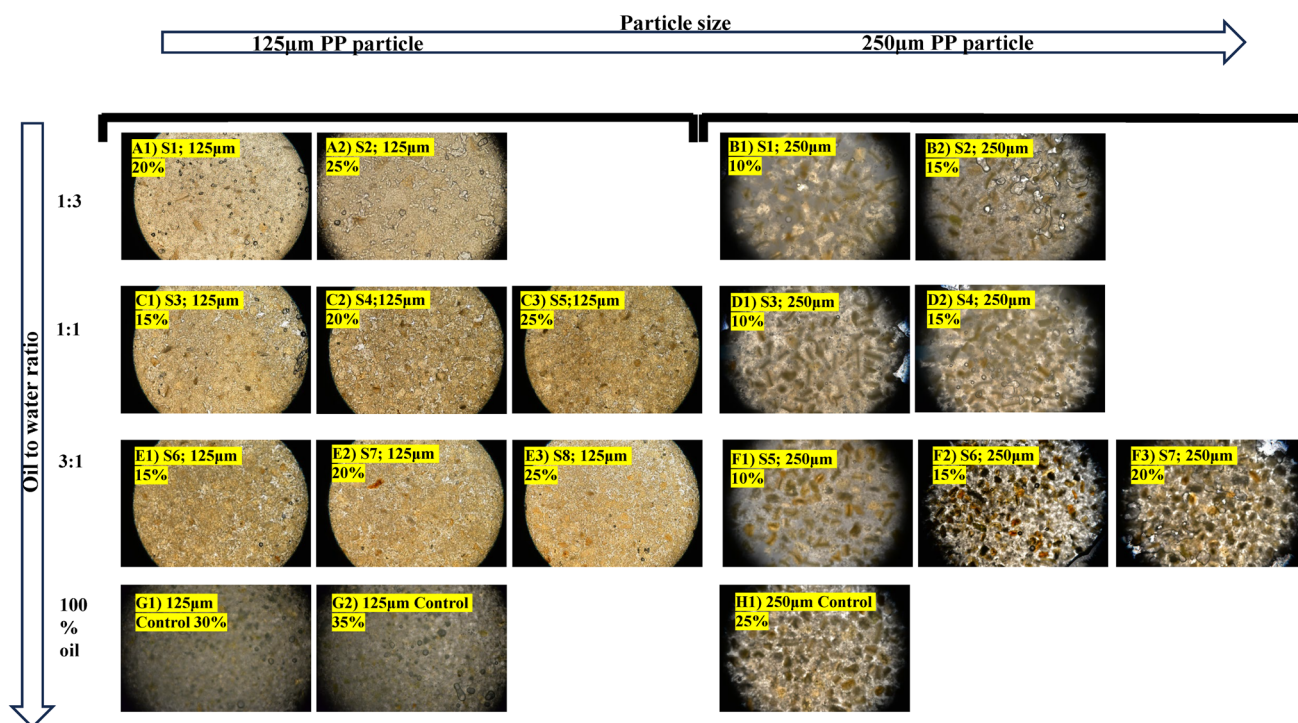
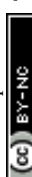


Fig. 3 Bright field microscopy images (40 times magnification) of sorbents produced using pomelo peel (PP) powders with varied particle sizes (125  $\mu\text{m}$  and 250  $\mu\text{m}$ ), oil-to-water ratios (1 : 3, 1 : 1, and 3 : 1), and PP powder concentrations (10–35% w/w). The left three columns represent sorbents formed from 125  $\mu\text{m}$  PP powder, while the right three columns represent those formed from 250  $\mu\text{m}$  PP powder. Four samples correspond to the 1 : 3 oil-to-water ratio (A1, A2, B1, and B2), five to the 1 : 1 ratio (C1–C3, D1, and D2), and six (E1–E3 and F1–F3) to the 3 : 1 ratio. The last row shows oil-only sorbents (control samples). Each subfigure specifies the particle size and PP powder concentration used for the respective sorbents (e.g., "125  $\mu\text{m}$  15%" indicates sorbents made from 125  $\mu\text{m}$  PP powder at a 15% concentration).



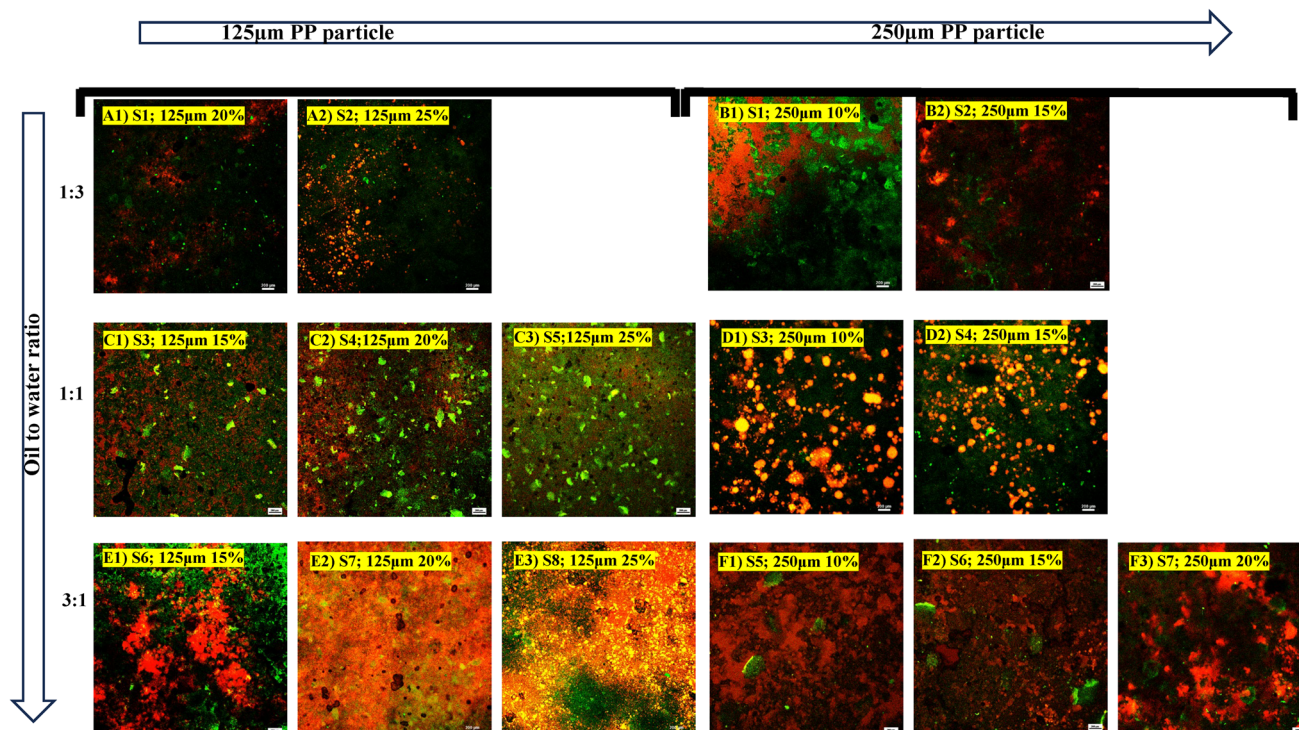


Fig. 4 CLSM micrographs (40 times magnification with a scale bar of 200  $\mu\text{m}$ ) of sorbents produced using pomelo peel (PP) powders with different particle sizes (125  $\mu\text{m}$  and 250  $\mu\text{m}$ ), oil-to-water ratios (1 : 3, 1 : 1, and 3 : 1), and PP powder concentrations (10–35% w/w). The left three columns represent sorbents formed from 125  $\mu\text{m}$  PP powder, while the right three columns represent those formed from 250  $\mu\text{m}$  PP powder. Four samples correspond to the 1 : 3 oil-to-water ratio (A1, A2, B1, and B2), five to the 1 : 1 ratio (C1–C3, D1, and D2), and six (E1–E3 and F1–F3) to the 3 : 1 ratio. The last row shows oil-only sorbents (control samples). Each subfigure specifies the particle size and PP powder concentration used for the respective sorbents (e.g., "125  $\mu\text{m}$  15%" indicates sorbents made from 125  $\mu\text{m}$  PP powder at a 15% concentration).

Table 1 Textural profile analysis and oil loss of self-sustained sorbents derived from pomelo peel powder (10–25%) with two particle sizes (250 and 125  $\mu\text{m}$ ), formed using an immediate setting emulsion approach with various oil-to-water ratios; control samples represent sorbents formed exclusively from PP powder and oil<sup>a</sup>

Sorbent samples	Oil : water ratios	PP conc.	Oil loss (%)	Hardness (N)	Cohesiveness (%)
<b>250 <math>\mu\text{m}</math> particle size</b>					
250 $\mu\text{m}$ S1	1 : 3	10%	5.38 $\pm$ 0.41 <sup>aC</sup>	0.55 $\pm$ 0.04 <sup>bC</sup>	51.02 $\pm$ 3.85 <sup>aA</sup>
250 $\mu\text{m}$ S2	1 : 3	15%	4.48 $\pm$ 2.00 <sup>aC</sup>	1.08 $\pm$ 0.15 <sup>bC</sup>	54.20 $\pm$ 2.86 <sup>aA</sup>
250 $\mu\text{m}$ S3	1 : 1	10%	32.14 $\pm$ 2.11 <sup>aB</sup>	1.02 $\pm$ 0.04 <sup>bA</sup>	34.58 $\pm$ 0.73 <sup>aB</sup>
250 $\mu\text{m}$ S4	1 : 1	15%	29.83 $\pm$ 0.57 <sup>aB</sup>	2.47 $\pm$ 0.05 <sup>bA</sup>	32.05 $\pm$ 0.83 <sup>aB</sup>
250 $\mu\text{m}$ S5	3 : 1	10%	50.80 $\pm$ 1.03 <sup>aA</sup>	0.84 $\pm$ 0.09 <sup>cB</sup>	35.71 $\pm$ 1.54 <sup>aB</sup>
250 $\mu\text{m}$ S6	3 : 1	15%	37.21 $\pm$ 1.51 <sup>bA</sup>	1.68 $\pm$ 0.06 <sup>cB</sup>	27.06 $\pm$ 1.45 <sup>bC</sup>
250 $\mu\text{m}$ S7	3 : 1	20%	20.07 $\pm$ 2.20 <sup>c</sup>	3.41 $\pm$ 0.12 <sup>b</sup>	29.15 $\pm$ 1.72 <sup>b</sup>
250 $\mu\text{m}$ control	1 : 0	25%	0.89 $\pm$ 0.04 <sup>d</sup>	25.40 $\pm$ 1.20 <sup>a</sup>	8.78 $\pm$ 1.02 <sup>c</sup>
<b>125 <math>\mu\text{m}</math> particle size</b>					
125 $\mu\text{m}$ S1	1 : 3	20%	22.40 $\pm$ 1.28 <sup>aB</sup>	0.49 $\pm$ 0.04 <sup>cA</sup>	26.63 $\pm$ 0.53 <sup>aA</sup>
125 $\mu\text{m}$ S2	1 : 3	25%	14.72 $\pm$ 0.36 <sup>cC</sup>	2.22 $\pm$ 0.12 <sup>cB</sup>	28.93 $\pm$ 2.54 <sup>aA</sup>
125 $\mu\text{m}$ S4	1 : 1	15%	36.05 $\pm$ 2.57 <sup>a</sup>	0.42 $\pm$ 0.11 <sup>c</sup>	28.77 $\pm$ 2.04 <sup>b</sup>
125 $\mu\text{m}$ S4	1 : 1	20%	25.19 $\pm$ 0.54 <sup>bB</sup>	1.01 $\pm$ 0.09 <sup>cB</sup>	27.90 $\pm$ 2.54 <sup>aA</sup>
125 $\mu\text{m}$ S5	1 : 1	25%	26.40 $\pm$ 1.22 <sup>bB</sup>	1.99 $\pm$ 0.01 <sup>cB</sup>	23.35 $\pm$ 0.23 <sup>aB</sup>
125 $\mu\text{m}$ S6	3 : 1	15%	35.63 $\pm$ 2.44 <sup>a</sup>	0.81 $\pm$ 0.02 <sup>d</sup>	21.21 $\pm$ 8.78 <sup>a</sup>
125 $\mu\text{m}$ S7	3 : 1	20%	25.19 $\pm$ 0.50 <sup>bB</sup>	2.36 $\pm$ 0.25 <sup>dA</sup>	16.07 $\pm$ 2.95 <sup>aB</sup>
125 $\mu\text{m}$ S8	3 : 1	25%	22.40 $\pm$ 1.21 <sup>bA</sup>	9.42 $\pm$ 1.42 <sup>cA</sup>	18.46 $\pm$ 1.04 <sup>aC</sup>
125 $\mu\text{m}$ control	1 : 0	30%	18.33 $\pm$ 0.52 <sup>c</sup>	12.98 $\pm$ 0.34 <sup>b</sup>	17.78 $\pm$ 0.51 <sup>a</sup>
125 $\mu\text{m}$ control	1 : 0	35%	6.82 $\pm$ 0.15 <sup>d</sup>	32.21 $\pm$ 2.28 <sup>a</sup>	16.97 $\pm$ 1.83 <sup>a</sup>

<sup>a</sup> Superscript capital letter(s) represent(s) statistically significant difference between different oil-to-water ratios, while lowercase letter(s) denote(s) statistically significant difference within the same particle size and oil-to-water ratio ( $P < 0.05$ ).



emulsion during fabrication significantly reduces the hardness of the sorbents as compared to the control samples absorbing rice bran oil only regardless of PP particle sizes and concentrations. The hardness values of emulsion-based/gel-like sorbents in this study fall within the range of 0.42 to 32.21 N, which is comparable with previous findings on candelilla wax, monoglycerides, egg-soybean protein isolate, monoacylglycerol and whey protein concentrate-based emulsions.<sup>6,23,29</sup> For 250  $\mu\text{m}$  sorbents, the control sample (25.40 N) was 7-fold harder than the hardest water-inclusive sorbents (250  $\mu\text{m}$  S7; 3.41 N). Similarly, 125  $\mu\text{m}$  sorbents with 30% oil content exhibited a hardness of 12.98 N, exceeding the hardness of all water-inclusive sorbents (ranging from 0.49 to 9.42 N).

The significant reduction in the hardness of sorbents *via* the emulsion-based method, compared to control samples absorbing only rice bran oil, can be attributed to several factors. In oil-only systems, PP particles rely entirely on particle-to-particle interactions to form a dense, rigid network. This compact structure contributes to the hardness of the sorbents.<sup>10,12</sup> In contrast, the inclusion of water in the emulsion

introduces a secondary phase (water droplets) that disrupts these direct interactions, leading to a less dense and more flexible network.<sup>29</sup> Water also hydrates and lubricates PP fibres, reducing interparticle friction and further decreasing hardness.<sup>30,31</sup> In emulsion-based systems, the heterogeneous microstructure resulting from the distribution of oil and water creates a soft and less rigid structure due to the interaction of PP particles, oil droplets, and water droplets, regardless of the PP particle size or concentration.<sup>30,31</sup> In this study, it is also observed that increasing the PP powder concentration enhanced the hardness of the sorbents. This is due to the filling effects of PP particles, which is widely reported in past studies.<sup>9-13</sup> These findings highlight how emulsion-based fabrication methods significantly impact the textural properties of PP-based sorbents, offering opportunities to tailor their functionality for specific applications.

Cohesiveness measured by TPA refers to the degree to which a material can withstand a second deformation relative to its first, providing a measure of its internal bonding strength and elasticity during compression.<sup>32</sup> In summary, the additional

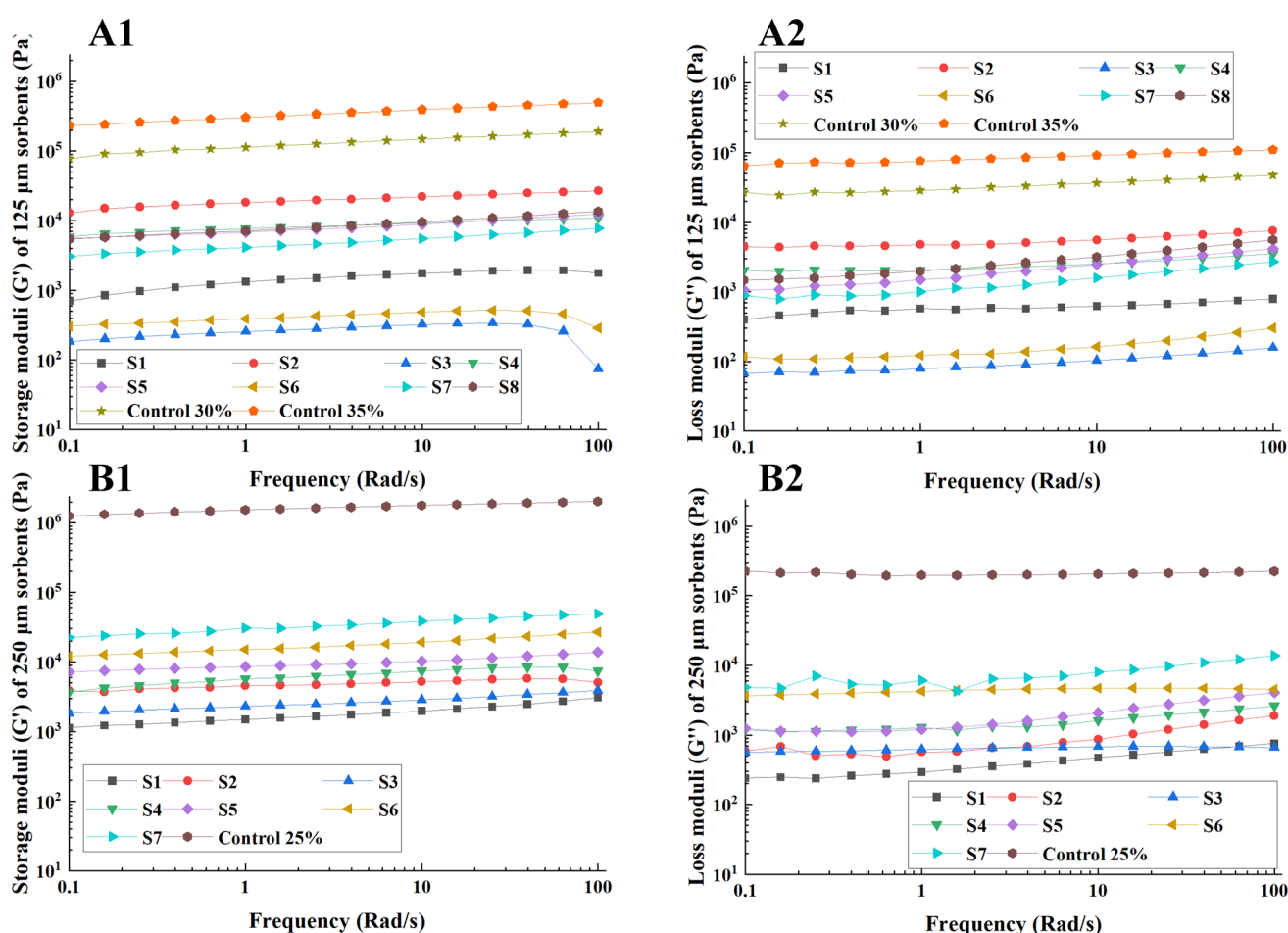


**Fig. 5** Frequency sweeping test of sorbents produced using pomelo peel (PP) powders with different particle sizes (125  $\mu\text{m}$  and 250  $\mu\text{m}$ ), oil-to-water ratios (1 : 3, 1 : 1, and 3 : 1), and PP powder concentrations (10–35% w/w); storage moduli (A1) and loss moduli (A2) of 8 sorbent samples (S1–S8) formed from 125  $\mu\text{m}$  PP particles and 2 oil-only sorbents as control samples; storage moduli (B1) and loss moduli (B2) of 7 sorbent samples (S1–S7) formed from 250  $\mu\text{m}$  PP particles and 1 oil-only sorbent as the control sample; details of PP powder concentrations and oil-to-water ratios are presented in Appendix 1.

water phase significantly enhances the cohesiveness of most sorbents (Table 1), which can be attributed to enhanced hydration, elasticity, and balanced microstructure provided by the inclusion of water.<sup>30</sup> The cohesiveness decreased as the oil-to-water ratio increased. This may be due to the hydration of PP fibres in water-rich systems, which enhances the flexibility and recovery after deformation, whereas oil-only sorbents lack this hydration, resulting in brittleness.<sup>12,33</sup> Water droplets in the sorbents can act as “bridges” between PP particles, strengthening interparticle interactions and leading to a more interconnected network formed by physical bonds.<sup>34</sup> These water-mediated connections contribute to a more cohesive and elastic network, as opposed to oil-only systems, where interactions are primarily hydrophobic and less flexible. The results obtained are in accordance with our previous study which demonstrated that PP-based hydrogel-like sorbents exhibit high cohesiveness, while PP-based oleogel-like sorbents are characterised by high hardness. In this study, the produced sorbents contained both water and oil phases, and the inclusion of water creates a more balanced microstructure with both hydrophilic and hydrophobic interactions, supporting higher TPA cohesiveness compared to the more rigid, hydrophobic-dominated structure of oil-only sorbents.<sup>13</sup> However, at an oil-to-water ratio of 3 : 1, the 125 µm sorbents (Tables 1 and S6–S8†) showed no improvement in cohesiveness, indicating that insufficient water limits network formation, which leads to a structure similar to oil-only sorbents.<sup>29</sup>

The rheological data showed a similar trend with the hardness of the sorbents. Fig. 5 presents loss and storage moduli of all sorbents produced. Most sorbents exhibited a higher  $G'$  (storage modulus) value than  $G''$  (loss modulus) throughout the frequency sweep, except for 125 µm S3 and S6 samples, which displayed a different trend at the end of the test. This indicates that the majority of the sorbents possess gel-like behaviour and can be classified as strong gels.<sup>13</sup> However, the 125 µm S3 and S6 samples exhibited more emulsion-like characteristics, likely due to their lower PP powder content (15%). As discussed in the Microstructural analysis section, the PP powder plays a critical role in the structural integrity of 125 µm sorbents due to droplet-to-particle interactions. Reducing the PP powder content weakens the sorbents by resulting in a less cohesive structure and reduced filling effects.

The textural and rheological properties of the sorbents exhibited characteristics similar to those of traditional emulsion gels. For example, the  $\kappa$ -carrageenan and whey protein-based emulsion gel displayed a storage modulus ranging from  $10^2$  to  $10^4$ , which aligns with the findings of this study.<sup>6</sup> Additionally, candelilla wax-based emulsion gels demonstrated a hardness of 20–50 g, which also corresponds to the range observed in this research.<sup>29</sup> Thus, the emulsion-based/gel-like sorbents studied exhibit similar characteristics to traditional gels. In addition, it reduced the oil content compared to pure oleogel-like sorbents as we presented in past studies.<sup>12,13</sup> Furthermore, the cohesiveness of the sorbents significantly increased with the addition of water, a critical factor for food processing.<sup>35</sup> This feature highlights their potential to be developed into a convenient, healthy, and cost-effective fat replacer.

### 3.4 Oil loss

Oil loss is a key indicator of the functionality of a sorbent, particularly in terms of its stability, structural integrity, and suitability for specific applications. Table 1 presents that oil loss decreases when the concentration of PP powder is increased. For example, the oil loss of 250 µm sorbents at an oil-to-water ratio of 3 : 1 decreased from 50.80% to 20.07% in samples S5–S7 (10–20% PP powder). A similar trend was observed in 125 µm sorbents, where oil loss decreased from 35.63% to 22.40% in samples S6–S8 (15–25% PP powder). These findings align with the observations of El Gheriany *et al.*,<sup>26</sup> who noted that an increase in the gelator content enhanced the surface area for oil–water interactions, leading to reduced oil loss.

In contrast, as the oil phase became more dominant (e.g. with an oil-to-water ratio shifting from 1 : 3 to 3 : 1) both 125 and 250 µm sorbents exhibited increasing oil losses. For 250 µm sorbents, oil loss increased significantly from 5.38% (S1) to 50.80% (S5). A similar trend was seen in 125 µm sorbents, where oil loss increased from 14.72% (S2) to 22.40% (S8).

Most sorbents exhibited an oil loss of 20–30%, while some, such as 250 µm S5, demonstrated a significantly higher oil loss of up to 50%, which compromises stability during processing. Liu *et al.*<sup>21</sup> reported that sorghum wax-based oleogels have an oil loss rate of 20–30%. Therefore, 250 µm S5 and S6 samples may not be suitable for food processing applications. Future studies should focus on 250 µm S7 and 125 µm S6–S8 samples, as they

**Table 2** Oil droplet sizes of self-sustained sorbents derived from pomelo peel powder (10–25%) with two particle sizes (250 and 125 µm), formed using an immediate setting emulsion approach with various oil-to-water ratios; control samples represent sorbents formed exclusively from PP powder and oil<sup>a</sup>

Sorbent samples	Oil : water ratios	PP concentration	$D_{4,3}$ (µm)
<b>250 µm particle size</b>			
250 µm S1	1 : 3	10%	$357.40 \pm 2.19^{\text{aA}}$
250 µm S2	1 : 3	15%	$274.40 \pm 3.83^{\text{bA}}$
250 µm S3	1 : 1	10%	$246.20 \pm 3.83^{\text{bB}}$
250 µm S4	1 : 1	15%	$182.64 \pm 10.03^{\text{bC}}$
250 µm S5	3 : 1	10%	$241.20 \pm 6.38^{\text{cC}}$
250 µm S6	3 : 1	15%	$202.20 \pm 2.59^{\text{bB}}$
250 µm S7	3 : 1	20%	$166.26 \pm 3.63^{\text{cC}}$
250 µm control	1 : 0	25%	$230.21 \pm 19.06^{\text{cC}}$
<b>125 µm particle size</b>			
125 µm S1	1 : 3	20%	$128.60 \pm 1.36^{\text{aA}}$
125 µm S2	1 : 3	25%	$115.82 \pm 3.76^{\text{bA}}$
125 µm S4	1 : 1	15%	$126.80 \pm 0.75^{\text{aA}}$
125 µm S4	1 : 1	20%	$114.20 \pm 0.75^{\text{aB}}$
125 µm S5	1 : 1	25%	$77.04 \pm 3.68^{\text{dC}}$
125 µm S6	3 : 1	15%	$95.06 \pm 4.74^{\text{bB}}$
125 µm S7	3 : 1	20%	$95.22 \pm 3.91^{\text{bC}}$
125 µm S8	3 : 1	25%	$82.24 \pm 2.21^{\text{cB}}$
125 µm control	1 : 0	30%	$116.60 \pm 0.80^{\text{bB}}$
125 µm control	1 : 0	35%	$113.20 \pm 0.40^{\text{bB}}$

<sup>a</sup> Superscript capital letter(s) represent(s) statistically significant difference between different oil-to-water ratios, while lowercase letter(s) denote(s) statistically significant difference within the same particle size and oil-to-water ratio ( $P < 0.05$ ).

demonstrate similarities to emulsion gels and exhibit low oil loss.

### 3.5 Oil droplet size and the impacts of water

Table 2 presents the oil droplet sizes in emulsion gel-like sorbents, indicating that the sorbents with a particle size of 250  $\mu\text{m}$  have larger oil droplets compared to those with a particle size of 125  $\mu\text{m}$ . Specifically, the  $D_{4,3}$  values for the 250  $\mu\text{m}$  and 125  $\mu\text{m}$  sorbents range from 166.26 to 357.40  $\mu\text{m}$  and from 77.04 to 128.60  $\mu\text{m}$ , respectively. The particle size measurement results align well with the microstructural observation under a confocal laser scanning microscope in which 125  $\mu\text{m}$  sorbents contained numerous smaller particles compared to 250  $\mu\text{m}$  sorbents (Fig. 4). Additionally, the oil droplet size showed a tendency to decrease as the oil phase concentration increased. For instance, when the oil-to-water ratio increased from 1 : 3 to 3 : 1, the oil droplet size of the 250  $\mu\text{m}$  sorbents (with 10% PP content) decreased from 357.40  $\mu\text{m}$  to 241.20  $\mu\text{m}$ . A similar trend was observed for the 125  $\mu\text{m}$  sorbents. In this case, as the oil-to-water ratio increased from 1 : 3 to 3 : 1, the oil droplet size of the 125  $\mu\text{m}$  sorbents (with 20% oil content) reduced from 128.60  $\mu\text{m}$  to 95.22  $\mu\text{m}$ . This tendency occurs because a higher oil phase concentration increases the emulsion viscosity, creating a more structured system with densely packed oil droplets, which ultimately lead to a reduction in oil droplet size.<sup>36</sup> Additionally, the wetting of PP particles

induces steric hindrance, which limits the flocculation and coalescence of oil droplets, thereby reducing their size.<sup>37</sup>

An increase in PP powder content also led to a reduction in oil droplet size within the sorbents. For example, at an oil-to-water ratio of 3 : 1, the  $D_{4,3}$  value of 250  $\mu\text{m}$  sorbents decreased from 241.20  $\mu\text{m}$  (250  $\mu\text{m}$  S5 sample) to 166.26  $\mu\text{m}$  (250  $\mu\text{m}$  S7 sample). A similar trend was observed in 125  $\mu\text{m}$  sorbents, where the droplet size decreased from 95.06  $\mu\text{m}$  (125  $\mu\text{m}$  S6 sample) to 82.24  $\mu\text{m}$  (125  $\mu\text{m}$  S8 sample) at the same oil-to-water ratio. The reduction in particle size signifies a more dispersed oil-in-water system. Previous studies on bigel systems have shown that smaller particle sizes result in harder gels due to the increased viscosity and enhanced textural properties of the bigels.<sup>38,39</sup>

### 3.6 Oxidative stability and phenolic content of emulsion-based/gel-like sorbents

The oxidative stability of the produced sorbents is critical for their potential application as fat replacers. In this study, all water-rich sorbents (oil-to-water ratios of 1 : 3 and 1 : 1) fail the oxidative stability test due to visible mold growth after 2 days of storage at the accelerated temperature (50  $\pm$  1  $^{\circ}\text{C}$ ). This can be partly attributed to the nutrient-rich composition of the PP powder, which provides an excellent substrate for mold growth when combined with high moisture levels.<sup>40</sup> Additionally, the gel matrix of the sorbents, formed from the PP powder, may not

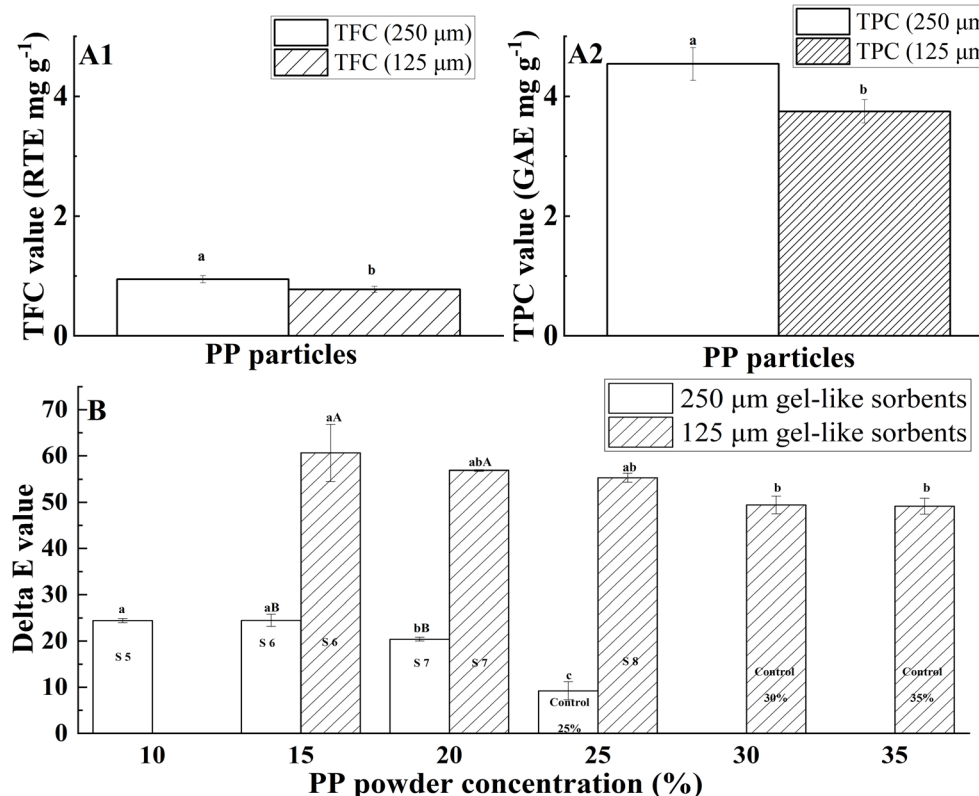


Fig. 6 (A1) Total flavonoid content (TFC) and (A2): total phenolic content (TPC) of pomelo peel (PP) powders (125  $\mu\text{m}$  & 250  $\mu\text{m}$ ); (B)  $\Delta E$  values of sorbents produced using pomelo peel (PP) powders with different particle sizes (125  $\mu\text{m}$  and 250  $\mu\text{m}$ ) formed at a 3 : 1 oil-to-water ratio during the 10 day accelerated storage test at 50  $^{\circ}\text{C}$ , where blank bars and bars with backslashes represent  $\Delta E$  values of 250  $\mu\text{m}$  PP-based sorbents and 125  $\mu\text{m}$  PP-based sorbents, respectively.



effectively bind, or immobilise all the water, leaving some free water available to support microbial activity.<sup>41</sup> As a result, only the oil-rich sorbents were evaluated for oxidative stability, and the phenolic content was determined to evaluate their resistance to oxidation in relation to their inherent phenolic compounds.

Fig. 6(A1 & A2) show the total phenolic content (TPC) and total flavonoid content (TFC) of PP powder, which are significantly influenced by particle size. Specifically, 250  $\mu\text{m}$  PP particles exhibit significantly higher TPC (4.54 vs. 3.75 GAE mg  $\text{g}^{-1}$ ) and TFC (0.95 vs. 0.78 RTE mg  $\text{g}^{-1}$ ) values compared to 125  $\mu\text{m}$  particles. This difference is likely due to the increased surface area of smaller particles, which makes them more prone to oxidation during grinding.<sup>42</sup> PP powder used in this study contains a higher phenolic and flavonoid content than other plant products, such as sorghum pericarp (4.13 GAE mg  $\text{g}^{-1}$ ).<sup>43</sup> These compounds are natural antioxidants with potential health benefits, including anticancer, anti-inflammatory, and anti-aging properties. The high antioxidant capacity of PP powder further enhances the health benefits of its use as a fat replacer.<sup>44</sup> Moreover, the high levels of phenolics and flavonoids in PP can influence lipid oxidation and colour stability of sorbents during storage. The TPC and TFC of rice bran oil were also tested and found to be negligible (less than 0.1 GAE mg  $\text{g}^{-1}$  and 0.01 RTE mg  $\text{g}^{-1}$ , respectively). This indicates that the antioxidants in PP powders are the major contributors to the

oxidative stability of the sorbent systems. While a high phenolic content may provide potential health benefits and help delay lipid oxidation, it can also impart bitterness, which may compromise the sensory acceptability of the product.<sup>45</sup> Therefore, it is crucial to optimise the fat replacement ratio, particularly if this sorbent system is intended for use in food formulations, to balance functionality with sensory quality associated with the incorporation of PP powder.<sup>46</sup>

Fig. 7 presents the peroxide value (PV) and *p*-anisidine value (PAV) of all sorbents (oil-to-water ratio 3 : 1) studied. The peroxide value measures the primary oxidative products, while the *p*-anisidine value quantifies the secondary oxidative products derived from the primary ones. Sorbents with 250  $\mu\text{m}$  particles exhibited better oxidative stability compared to those with 125  $\mu\text{m}$  particles, as indicated by lower PV and PAV values. This enhanced stability is likely attributed to the higher phenolic and flavonoid contents in the 250  $\mu\text{m}$  PP powders, which delayed the oxidation of the sorbents. These antioxidants impede lipid peroxidation through their chelating properties, free radical scavenging abilities, and capacity to neutralise carbonyl compounds.<sup>47</sup>

Moreover, the PP powder content was inversely related to lipid peroxidation for sorbents of the same particle size. For example, the 125  $\mu\text{m}$  S6 sample exhibited the highest PV and PAV. This is because increasing the concentration of PP powder enhances the antioxidant effect.<sup>48</sup> The PV of the 125  $\mu\text{m}$  S6

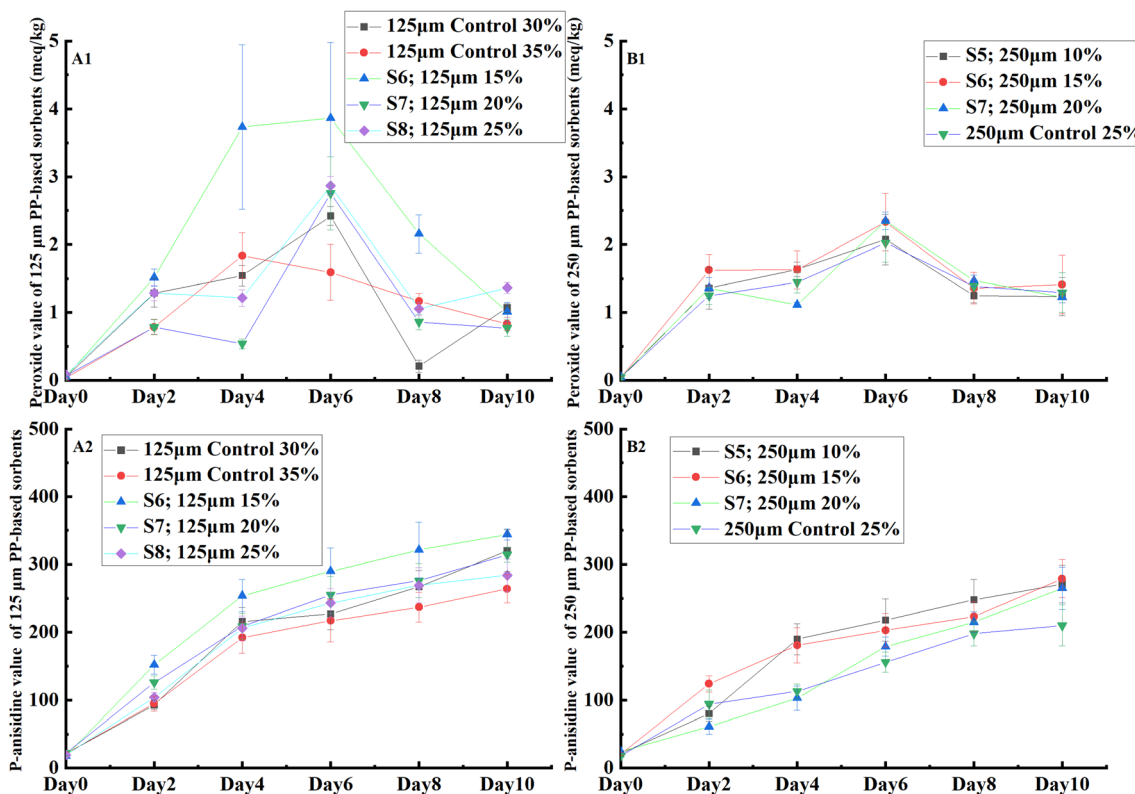


Fig. 7 Peroxide value (PV) and *p*-anisidine value (PAV) of sorbents formed at a 3 : 1 oil-to-water ratio from pomelo peel (PP) powder (125  $\mu\text{m}$  and 250  $\mu\text{m}$ ) during a 10 day accelerated storage test. Panels A1 and A2 show PV and PAV values, respectively, for 125  $\mu\text{m}$  sorbents (S6, S7, and S8) and two oil-only control samples. Panels B1 and B2 show PV and PAV values, respectively, for 250  $\mu\text{m}$  sorbents (S5, S6, and S7) and one oil-only control sample. Detailed compositions of all samples are provided in Appendix 1.



sample appears to exhibit a large standard deviation at the early stage, indicating high oxidative instability. This remarkable variation suggests that the 125  $\mu\text{m}$  S6 sample, which contains a lower concentration of PP powder, may be unsuitable for long-term storage.<sup>49</sup> In contrast, samples containing higher PP concentrations (20–25%) formed a denser gel matrix, effectively entrapping oil droplets and reducing oxygen permeability, which collectively improved the oxidative stability, further limiting lipid peroxidation.<sup>50</sup>

Fig. 6B shows the  $\Delta E$  values of sorbents during storage. The colour stability of sorbents is primarily governed by PP particle size. For instance, at 15% PP content, 125  $\mu\text{m}$  S6 showed a  $\Delta E$  value of 24.49 which is significantly lower than 250  $\mu\text{m}$  S6 which had a  $\Delta E$  value of 60.67. As mentioned before, this is due to the lower phenolic and flavonoid contents of 125  $\mu\text{m}$  than 250  $\mu\text{m}$  PP powder. Similarly, increasing the PP content also decreased the  $\Delta E$  value by enhancing the total antioxidant capacity. Besides, a small particle size accelerated the pigment oxidation due to its large surface area and the resulting high  $\Delta E$  value.<sup>51</sup>

The stability test of the selected sorbents demonstrated high oxidative stability. Generally, the peroxide value (PV) should not exceed 10 during storage to ensure product quality. All samples in this study maintained PV values below this threshold, indicating that these sorbents possess sufficient stability for practical applications.<sup>52</sup> Therefore, these sorbents show strong potential as fat replacers due to their high oxidative stability.

## 4 Conclusion

This study successfully developed emulsion-based gel-like sorbents using pomelo peel (PP) powder with particle sizes of 125  $\mu\text{m}$  and 250  $\mu\text{m}$ . The sorbents, formed through an oil-water emulsion approach, exhibited properties that are influenced by oil-to-water ratios, particle sizes, and PP powder concentrations. Compared to oil-only sorbents, the emulsion-based sorbents required less PP powder and reduced overall oil content, providing a healthier alternative. Adding a water phase significantly impacted the sorbents' structural integrity, texture, rheology, and oil retention. While the water phase reduced hardness by disrupting the dense network of oil-only systems and improving the cohesiveness through enhanced fibre hydration, it also increased oil loss and introduced free water, heightening mold susceptibility. This trade-off highlights the balance between texture and stability. Adjusting the oil-to-water ratio, PP particle size, and powder concentration allows customisation of the sorbents' structural and functional properties, positioning PP-based sorbents as versatile and sustainable fat replacers. Their similarity to traditional gel-based fat replacers suggests potential applications in meat, bakery, and confectionery products. Future research should further explore the application of these emulsion gel-like sorbents, focusing on their impact on sensory attributes and processing characteristics across diverse food systems.

## Appendix

Appendix 1. Formulations of the produced sorbents made with pomelo peel (PP) powders of varied particle sizes (125 and 250  $\mu\text{m}$ ) and various oil : water ratios.

Sample names	PP powder particle size	Oil : water ratios	PP powder (%)	Oil (%)	Water (%)
S1	250 $\mu\text{m}$	1 : 3	10.0	22.50	67.50
S2	250 $\mu\text{m}$	1 : 3	15.0	21.25	63.75
S3	250 $\mu\text{m}$	1 : 1	10.0	45.00	45.00
S4	250 $\mu\text{m}$	1 : 1	15.0	42.50	42.50
S5	250 $\mu\text{m}$	3 : 1	10.0	67.50	22.50
S6	250 $\mu\text{m}$	3 : 1	15.0	63.75	21.25
S7	250 $\mu\text{m}$	3 : 1	20.0	60.00	20.00
<i>Control 25% 250 <math>\mu\text{m}</math></i>		<i>1 : 0</i>	25.0	75.00	N/A
S1	125 $\mu\text{m}$	1 : 3	20.0	20.00	60.00
S2	125 $\mu\text{m}$	1 : 3	25.0	18.75	56.25
S3	125 $\mu\text{m}$	1 : 1	15.0	42.50	42.50
S4	125 $\mu\text{m}$	1 : 1	20.0	40.00	40.00
S5	125 $\mu\text{m}$	1 : 1	25.0	37.50	37.50
S6	125 $\mu\text{m}$	3 : 1	15.0	63.75	21.25
S7	125 $\mu\text{m}$	3 : 1	20.0	60.00	20.00
S8	125 $\mu\text{m}$	3 : 1	25.0	56.25	18.75
<i>Control 30% 125 <math>\mu\text{m}</math></i>		<i>1 : 0</i>	30.0	70.00	N/A
<i>Control 35% 125 <math>\mu\text{m}</math></i>		<i>1 : 0</i>	35.0	65.00	N/A

## Data availability

The data supporting this article have been included as part of the ESI.<sup>†</sup>

## Author contributions

Haoxin Wang: data curation, formal analysis, investigation, writing – original draft. Peng Wang: supervision, writing – review & editing. Stefan Kasapis: supervision, writing – review & editing; Tuyen Truong: conceptualization, supervision, writing – original draft, writing – review & editing.

## Conflicts of interest

All authors declare no competing financial interest.

## Acknowledgements

The authors would like to thank the administrative and technical support at RMIT University. Additionally, the first author acknowledges the scholarship provided to the student by RMIT University.

## References

- 1 Y. Ren, L. Huang, Y. Zhang, H. Li, D. Zhao, J. Cao, *et al.*, Application of emulsion gels as fat substitutes in meat products, *Foods*, 2019, **13**, 1950.
- 2 S. Li, G. Chen, X. Shi, C. Ma and F. Liu, Comparative study of heat- and enzyme-induced emulsion gels formed by gelatin





and whey protein isolate: physical properties and formation mechanism, *Gels*, 2022, **8**, 212.

3 B. Wang, P. Wang, X. Xu and G. Zhou, Structural transformation of egg white protein particles modified by preheating combined with pH-shifting: mechanism of enhancing heat stability, *LWT-Food Sci. Technol.*, 2022, **170**, 114114.

4 A. Martín-Illana, F. Notario-Pérez, R. Cazorla-Luna, R. Ruiz-Caro, M. C. Bonferoni, A. Tamayo, *et al.*, Bigels as drug delivery systems: from their components to their applications, *Drug Discovery Today*, 2022, **27**, 1008–1026.

5 C. Liu, Z. Zheng, Y. Shi, Y. Zhang and Y. Liu, Development of low-oil emulsion gel by solidifying oil droplets: roles of internal beeswax concentration, *Food Chem.*, 2021, **345**, 128811.

6 A. Habibi, C. Dekiwadia, S. Kasapis and T. Truong, Fabrication of double emulsion gel using monoacylglycerol and whey protein concentrate: the effects of primary emulsion gel fraction and particle size, *J. Food Eng.*, 2023, **341**, 111350.

7 A. J. Gravelle, A. G. Marangoni and S. Barbut, Modulating water mobility in comminuted meat protein gels using model hydrophilic filler particles, *LWT-Food Sci. Technol.*, 2020, **129**, 109376.

8 S. A. Salami, G. Luciano, M. N. O'Grady, L. Biondi, C. J. Newbold, J. P. Kerry, *et al.*, Sustainability of feeding plant by-products: a review of the implications for ruminant meat production, *Anim. Feed Sci. Technol.*, 2019, **251**, 37–55.

9 Z. Lu, F. Ye, G. Zhou, R. Gao, D. Qin and G. Zhao, Micronized Apple Pomace as a novel emulsifier for food o/w pickering emulsion, *Food Chem.*, 2020, **330**, 127325.

10 A. David, M. David, P. Lesniarek, E. Corfias, Y. Pululu, M. Delample, *et al.*, Oleogelation of rapeseed oil with cellulose fibers as an innovative strategy for palm oil substitution in chocolate spreads, *J. Food Eng.*, 2021, **292**, 110315.

11 J. Gao, Y. Qiu, F. Chen, L. Zhang, W. Wei, X. An, *et al.*, Pomelo peel derived nanocellulose as Pickering stabilizers: fabrication of pickering emulsions and their potential as sustained-release delivery systems for lycopene, *Food Chem.*, 2023, **415**, 135742.

12 H. Wang, P. Wang, S. Kasapis and T. Truong, Optimising corn (*zea mays*) cob powder as an effective sorbent for diverse gel matrices: exploring particle size and powder concentration effects, *Int. J. Food Sci. Technol.*, 2024, **59**(9), 6628–6641.

13 H. Wang, P. Wang, S. Kasapis and T. Truong, Pomelo (*citrus grandis* L.) peels as effective sorbents for diverse gel matrices: the influence of particle size and powder concentration, *J. Food Eng.*, 2024, **370**, 111966.

14 M. Hörmann-Wallner, R. Krause, B. Alfaro, H. Jilani, M. Laureati, V. L. Almli, *et al.*, Intake of fibre-associated foods and texture preferences in relation to weight status among 9–12 years old children in 6 European countries, *Front. Nutr.*, 2021, **8**, 633807.

15 R. Tocmo, J. Pena-Fronteras, K. F. Calumba, M. Mendoza and J. J. Johnson, Valorization of Pomelo (*citrus grandis* osbeck) peel: a review of current utilization, phytochemistry, bioactivities, and mechanisms of action, *Compr. Rev. Food Sci. Food Saf.*, 2020, **19**(4), 1969–2012.

16 T. T. Ha, T. N. Mai, T. T. Tran, N. H. Nguyen, T. D. Le and V. M. Nguyen, Antioxidant activity and inhibitory efficacy of citrus *grandis* peel extract against carbohydrate digestive enzymes *in vitro*, *Food Sci. Technol.*, 2022, **42**, 109721.

17 V. L. Singleton and J. A. Rossi, Colorimetry of total phenolics with phosphomolybdic-phosphotungstic acid reagents, *Am. J. Enol. Vitic.*, 1965, **16**(3), 144–158.

18 H. Wang, H. Sun, P. Zhang and Z. Fang, Effects of processing on the phenolic contents, antioxidant activity and volatile profile of Wheat Bran Tea, *Int. J. Food Sci. Technol.*, 2019, **54**(12), 3156–3165.

19 M. Singh, T. Thrimawithana, R. Shukla and B. Adhikari, Extraction and characterization of polyphenolic compounds and potassium hydroxycitrate from *Hibiscus Sabdariffa*, *J. Future Foods*, 2021, **4**, 100087.

20 N. Luo, A. Ye, F. M. Wolber and H. Singh, In-mouth breakdown behaviour and sensory perception of emulsion gels containing active or inactive filler particles loaded with capsaicinoids, *Food Hydrocolloids*, 2020, **108**, 106076.

21 L. Liu, I. S. Ramirez, J. Yang and O. N. Ciftci, Evaluation of oil-gelling properties and crystallization behavior of sorghum wax in fish oil, *Food Chem.*, 2020, **309**, 125567.

22 W. Zuo, X. Hu, Y. Yang, L. Jiang, L. Ren and H. Huang, Development of an improved method to determine saturated aliphatic aldehydes in docosahexaenoic acid-rich oil: a supplement to p-anisidine value, *Eur. J. Lipid Sci. Technol.*, 2017, **119**(12), 1700243.

23 M. Zhang, Y. Yang and N. C. Acevedo, Effect of oil content and composition on the gelling properties of egg-SPI proteins stabilized emulsion gels, *Food Biophys.*, 2020, **15**(4), 473–481.

24 E. Dickinson, Hydrocolloids as emulsifiers and emulsion stabilizers, *Food Hydrocolloids*, 2009, **23**(6), 1473–1482.

25 Y. Jia, C. Wang, I. Khalifa, Y. Zhu, Z. Wang, H. Chen, *et al.*, Pectin: a review with recent advances in the emerging revolution and multiscale evaluation approaches of its emulsifying characteristics, *Food Hydrocolloids*, 2024, **157**, 110428.

26 I. A. El Gheriany, F. Ahmad El Saqa, A. Abd El Razek Amer and M. Hussein, Oil spill sorption capacity of raw and thermally modified Orange Peel Waste, *Alexandria Eng. J.*, 2020, **59**(2), 925–932.

27 M. A. Mahmoud, Oil spill cleanup by raw flax fiber: modification effect, sorption isotherm, kinetics and thermodynamics, *Arabian J. Chem.*, 2020, **13**(6), 5553–5563.

28 Y. Kuang, Q. Xiao, Y. Yang, M. Liu, X. Wang, P. Deng, *et al.*, Investigation and characterization of Pickering emulsion stabilized by alkali-treated Zein (az)sodium alginate (SA) composite particles, *Materials*, 2023, **16**(8), 3164.

29 T. L. da Silva, D. B. Arellano and S. Martini, Effect of water addition on physical properties of emulsion gels, *Food Biophys.*, 2018, **14**(1), 30–40.

30 E. K. Gamstedt, Moisture induced softening and swelling of natural cellulose fibres in composite applications, *IOP Conf. Ser.: Mater. Sci. Eng.*, 2016, 2016139.

31 S.-W. Lo, T.-C. Yang, Y.-A. Cian and K.-C. Huang, A model for lubrication by oil-in-water emulsions, *J. Tribol.*, 2009, **132**(1), 11801.

32 A. J. Rosenthal and P. Thompson, What is cohesiveness?—a linguistic exploration of the food texture testing literature, *J. Texture Stud.*, 2021, **52**(3), 294–302.

33 M. L. García-Ortega, J. F. Toro-Vazquez and S. Ghosh, Development and characterization of structured water-in-oil emulsions with ethyl cellulose oleogels, *Food Res. Int.*, 2021, **150**, 110763.

34 E. Brini, C. J. Fennell, M. Fernandez-Serra, B. Hribar-Lee, M. Lukšić and K. A. Dill, How water's properties are encoded in its molecular structure and energies, *Chem. Rev.*, 2017, **117**(19), 12385–12414.

35 M. V. Chandra and B. A. Shamasundar, Texture profile analysis and functional properties of gelatin from the skin of three species of fresh water fish, *Int. J. Food Prop.*, 2014, **18**(3), 572–584.

36 T. Dapčević Hadnađev, P. Dokić, V. Krstonošić and M. Hadnađev, Influence of oil phase concentration on droplet size distribution and stability of oil-in-water emulsions, *Eur. J. Lipid Sci. Technol.*, 2013, **115**(3), 313–321.

37 S. M. Hodge and D. Rousseau, Flocculation and coalescence in water-in-oil emulsions stabilized by paraffin wax crystals, *Food Res. Int.*, 2003, **36**(7), 695–702.

38 L. Zeng, J. Lee, Y.-J. Jo and M.-J. Choi, Effects of micro- and nano-sized emulsions on physicochemical properties of emulsion–gelatin composite gels, *Food Hydrocolloids*, 2023, **139**, 108537.

39 M. L'Estimé, M. Schindler, N. Shahidzadeh and D. Bonn, Droplet size distribution in emulsions, *Langmuir*, 2023, **40**(1), 275–281.

40 B. Zaffora, L. Coisne and C. Gerard, Survival Models to Estimate Time to Visible Mold Growth on New Paper-Based Food-Contact Materials under Varying Environmental Conditions, *LWT-Food Sci. Technol.*, 2024, **193**(1), 115767.

41 H. Sawalha, R. den Adel, P. Venema, A. Bot, E. Flöter and E. van der Linden, Organogel-emulsions with mixtures of  $\beta$ -sitosterol and  $\gamma$ -Oryzanol: influence of water activity and type of oil phase on Gelling Capability, *J. Agric. Food Chem.*, 2012, **60**(13), 3462–3470.

42 J. Ferreira, K. Tkacz, I. P. Turkiewicz, M. I. Santos, A. Belas, A. Lima, *et al.*, Influence of particle size and extraction methods on phenolic content and biological activities of Pear Pomace, *Foods*, 2023, **12**(23), 4325.

43 S. Rao, A. B. Santhakumar, K. A. Chinkwo, G. Wu, S. K. Johnson and C. L. Blanchard, Characterization of phenolic compounds and antioxidant activity in sorghum grains, *J. Cereal Sci.*, 2018, **84**, 103–111.

44 C. Zehiroglu and S. B. Ozturk Sarikaya, The importance of antioxidants and place in today's scientific and Technological Studies, *J. Food Sci. Technol.*, 2019, **56**(11), 4757–4774.

45 K. Younis, S. Ahmad and M. A. Malik, Mosambi Peel Powder incorporation in meat products: effect on physicochemical properties and shelf life stability, *Appl. Food Res.*, 2021, **1**(2), 100015.

46 Y.-S. Choi, J.-H. Choi, D.-J. Han, H.-Y. Kim, H.-W. Kim, M.-A. Lee, *et al.*, Effects of laminaria japonica on the physico-chemical and sensory characteristics of reduced-fat pork patties, *Meat Sci.*, 2012, **91**(1), 1–7.

47 R. Zamora and F. J. Hidalgo, The triple defensive barrier of phenolic compounds against the lipid oxidation-induced damage in food products, *Trends Food Sci. Technol.*, 2016, **54**, 165–174.

48 S. Siriamornpun, E. Tangkhawanit and N. Kaewseejan, Reducing retrogradation and lipid oxidation of normal and glutinous rice flours by adding mango Peel Powder, *Food Chem.*, 2016, **201**, 160–167.

49 N. Gotoh and S. Wada, The importance of peroxide value in assessing food quality and food safety, *J. Am. Oil Chem. Soc.*, 2006, **83**(5), 473–474.

50 A. Ashkar, S. Laufer, J. Rosen-Kligvasser, U. Lesmes and M. Davidovich-Pinhas, Impact of different oil gelators and oleogelation mechanisms on digestive lipolysis of Canola Oil Oleogels, *Food Hydrocolloids*, 2019, **97**, 105218.

51 R. Martínez-Las Heras, A. Pinazo, A. Heredia and A. Andrés, Evaluation studies of Persimmon Plant (*diospyros kaki*) for physiological benefits and bioaccessibility of antioxidants by *in vitro* simulated gastrointestinal digestion, *Food Chem.*, 2017, **214**, 478–485.

52 A. Ismail, G. Bannenberg, H. B. Rice, E. Schutt and D. MacKay, Oxidation in EPA- and Dha-Rich Oils: an overview, *Lipid Technol.*, 2016, **28**(3–4), 55–59.

